

Variability of ionospheric total electron content at low-latitude station during twin solar maxima and solar minima of the 24th solar cycle and its comparison with different versions of IRI models

Mahesh Parwani^{1,*}, Azad Ahmad Mansoori², P. K. Sharma³ and P. K. Purohit⁴

¹Department of Physics, Barkatullah University, Bhopal 462 026, India

²Department of Physics, Govt. P.G. College, Tikagarh 472 001, India

³Barkatullah University Institute of Technology, Barkatullah University, Bhopal 462 026, India

⁴National Institute of Technical Teachers' Training and Research, Shamlu Hills, Bhopal 462 002, India

In this study, we compared the modelled total electron content (TEC), i.e. ionospheric TEC derived from the latest International Reference Ionosphere (IRI) versions (viz. IRI-2007, IRI-2012 and IRI-2016) with TEC derived by the International GNSS Service (IGS) receivers at a low-latitude station, namely Pathum Wan, Thailand (code-CUSV; lat. 13.74°N, long. 100.54°E) during the twin solar maxima 2012 and 2014, and the solar minima 2017 of the 24th solar cycle. We observed that the modelled TEC results were slightly underestimated than those derived by global positioning system (GPS), during the maxima and minima periods. It was also observed that the modelled TEC and GPS TEC followed a similar sinusoidal pattern with crests in the equinox months and troughs in the solstice months. We calculated standard deviation of the modelled TEC from the corresponding GPS TEC during the period. The study shows that the IRI model is more suitable when applied during solar minima period. We also carried out correlation study between modelled TEC and GPS TEC, and obtained a moderate degree of positive correlation. Thus we can conclude that IRI-2007 is the most suitable version for the twin solar maxima and the minima periods. Also IRI-2016 is the most suitable model for TEC estimation during geomagnetic storms.

Keywords: Geomagnetic storms, ionosphere, low-latitude station, solar cycle, total electron content.

NOWADAYS, many empirical models are being used to enhance the applicability of several scientific phenomena worldwide. Some of the commonly used empirical models are the Model for Earth's Atmosphere, International Geomagnetic Reference Field and Model for Earth's Magnetic Field, etc. The ionospheric counterpart of these

models is the International Reference Ionosphere (IRI). It is a globally recognized and accepted empirical model. This model was developed by the Committee on Space Research (COSPAR) and the International Union of Radio Science (URSI). It is a convenient gateway to specific ionospheric plasma parameters based on reliable data sources. Since the origin of the IRI model in 1969, it has been sustainably upgraded with the latest datasets and the advance modelling techniques¹. It had achieved great success along the way from the first version IRI-78 (ref. 2) to the latest version IRI-2016. During the course of time IRI-85, IRI-1990, IRI-2000, IRI-2007 and IRI-2012 versions have also been developed. The model provides monthly average of electron temperature and density, ion temperature and composition, including many other parameters from an altitude of 60–1500 km. It consists of a network of ionosondes around the globe that monitor ionospheric electron densities and the incoherent scatter radars that monitor plasma temperature, velocities and densities of the ionosphere. Unlike the theoretical model, working on the IRI model does not require any special understanding of the processes that constitute ionospheric plasma. The major drawback of the IRI model is that its results are dependent on the underlying database, which diminishes its reliability. Also, the regions and time periods are not well depicted in the database and these shortcomings reduce the accuracy of the model. This model is best suited, when applied to the continental mid-latitude region of the northern hemisphere, where we have the highest density of ionosondes. It is least suitable, when applied to the ocean areas where penetration of ionosondes is the least. This model is continuously upgraded with periodic workshops, wherein latest results are discussed and decisions about further updating are made. During the workshop at the US Air Force Academy in Colorado in 2009, a new effort was initiated to develop real-time IRI (RT-IRI)³. The worldwide data are gathered from the ground-based ionosondes,

*For correspondence. (e-mail: maheshkp.007.mp@gmail.com)

and space-based or satellite observations are used to improve the IRI model. As the result, we periodically get upgraded versions with advance features. For instance, the IRI-2016 model was updated with the latest parameters F2 peak height hmF2 and better representation of topside ion densities. The modification provides excellent opportunity to predict evening peak, which was not offered by previous versions. A significant modification has been made in the ion composition model, by lowering topside ionosphere transition height from 1000 to 600 km. Some features of solar indices data are also refurbished in the latest version⁴. The electromagnetic radiation of the sun ionizes the atmosphere and produces electron and positive ions that spread from 50 to 1000 km (ref. 5). These electrons and positive ions are generally equal in number, which forms an electrically neutral medium. This region is called ionosphere. It is responsible for ground-to-ground radio communication over long distances by means of the reflection of signals⁶. Ionosphere being a refractive medium also affects the propagation of trans-ionosphere electromagnetic signals that are responsible for ground-to-space radio communication. The global positioning system (GPS) signals on traversing through the ionosphere bear twin effect. It accelerates the propagation of carrier phase called phase advancement and slows down the propagation of codes by the same amount called group delay. This time delay is proportional to the density of electrons from the receiver to the satellite. The electron density in a unit cross-section area from the satellite to the receiver is known as slant total electron content (TEC). It is inversely proportional to the square of the frequency of propagation⁷⁻¹⁰. When the GPS signals pass through the ionosphere, they bear the signatures of this volatile medium. Thus the analysis of these signals provides information about the density of the constituents. With these results, global maps of ionospheric TEC are prepared for future references¹¹. In the last few decades, ionospheric TEC derived using IRI models and GPS satellites have been globally compared to estimate the performance of the IRI model at different latitudes, seasons and time periods. On the basis of these studies many theories have been established that provide an opportunity to estimate the performance of various IRI models^{12,13}. Some of the theories claim that IRI model overestimates seasonal and monthly TEC variations during both high and low solar activity periods. Some studies claim that performance of the model is better during low solar activity period than high solar activity period¹⁴. It was also reported that modelled TEC and GPS TEC show better correlation in high-latitude regions than at low- or mid-latitude regions⁴. Some researchers found that the modelled TEC data shows variation from corresponding data derived from IRI models¹⁵⁻¹⁷.

Due to our extensive dependency on GPS-based applications, precise predictions of ionospheric TEC are imperative for trouble-free GPS communication and ranging. For this, continuous technical upgradation and mathema-

tical modelling are needed¹⁸; but there are some limitations with GPS-based estimation techniques. The first is the limited number of IGS stations; most of them are spread in the northern hemispheric region only. The other limitation is the numerous errors and biases which occur when the signals travel over large distances, i.e. 20,200 km from the satellite to the receiver. So there is an urgent need among the scientific community to develop alternative, reliable, ground-based models for the study of the ionosphere. Thus, we opted to study the IRI model and the main aim of this study was to choose the best version of the IRI model. The reason for this is to estimate TEC variability during twin solar maxima 2012 and 2014 and solar minima 2017, so that the suitable version can be applied when GPS data are scarcely available.

Data description and analysis

The study was carried out with three types of datasets: ionospheric TEC data derived by GPS, TEC data derived by IRI model and geomagnetic index data (viz. Dst index (disturbance storm time index) and Bz component of interplanetary magnetic field) downloaded from Space Physics Data Facility OMNI website (<http://omniweb.gsfc.nasa.gov/>). We had considered a low-latitude IGS (International GPS Service) station, namely Pathum Wan, Thailand (code-CUSV), lat. 13.74°N and long. 100.54°E. For time references, universal time (UT) was considered.

Ionospheric TEC derived by GPS

We compared the modelled TEC with GPS-derived TEC (CUSV VTEC) during twin solar maxima 2012 and 2014 and solar minima 2017 of the 24th solar cycle. The GPS-derived TEC data of the chosen station were obtained from GPS receivers spread across the world and recorded data at periodic intervals. These recorded data are made freely available to all users by IGS. The data can be downloaded from <http://sopac.ucsd.edu/dataArchive/>. The data are provided in RINEX (receiver independent exchange) format, which is an internationally accepted data exchange format. It is in the standard ASCII format (i.e. readable text). The temporal resolution of the data is commonly 30 sec. The downloaded raw data were further processed using the scientific software developed by Gopi Krishna Seemala (Indian Institute of Geomagnetism (IIG), Navi Mumbai, India). This software reads the raw data from international GNSS Services (IGS) code file and provides the final readable data for further analysis¹⁹⁻²¹.

TEC data obtained from International Reference Ionosphere

IRI is a standard empirical model of the ionosphere. The model gives average values of electron content, electron

temperature and its density, ion temperature and ion composition as a function of local time, position and height²². In the present study, we have chosen IRI-2007, IRI-2012 and IRI-2016 models for comparison with GPS TEC. It is an international project sponsored by COSPAR and URSI. The IRI model calculates TEC by integrating electron density profile from a lower boundary to the specified upper boundary. According to the recommendations of CCIR (option for continental areas) and URSI (option for over-the ocean areas)^{23,24}, in this study we have examined the discrepancies between various IRI models and GPS observations. We have used TEC from various IRI models at the Pathum Wan station.

The on-line IRI model data for the considered versions were downloaded from <http://irimodel.org/>. We chose the upper boundary altitude 2000 km topside electron density option NeQuick and ABT 2009 for bottom thickness as the input parameter.

Geomagnetic index

In the present study, we have chosen Dst index to observe geomagnetic storms during the twin solar maxima and solar minima. Geomagnetic storm is a period of significant energy transfer from solar wind to magnetosphere. This energy transfer reshapes the magnetosphere; this reshaping process is known as geomagnetic storm. It depends on a number of factors such as solar wind speed, orientation of IMF B_z and its impact on the magnetosphere. The intensity and occurrence of a geomagnetic storm are measured on the Dst scale. Its quiet time value is between +20 to -20 nT. Further decrease in values indicate weakened geomagnetic field. On the Dst scale, geomagnetic storms can be classified as moderate (-50 to -100 nT), intense storm (-100 to -250 nT) and super storms (more than -250 nT). Another important factor is the interplanetary magnetic field (IMF). It is an important component in solar wind interaction with the geomagnetosphere. IMF is a vector quantity that has three components, B_x , B_y and B_z . B_x and B_y are not important for auroral activity as they are oriented parallel to the ecliptic, but B_z being perpendicular to the ecliptic is important for the study of geomagnetic storms. The southward magnetic field component B_z exhibits transfer of solar wind energy into the magnetosphere of the Earth. The southward IMF B_z is responsible for geomagnetic storms. We have downloaded the indices data from the Space Physics Data Facility OMNI (<http://omniweb.gsfc.nasa.gov/>). These are a daily data that can directly be used for the study of storms.

Results and discussion

The ionospheric TEC variation found to be related with the changing solar phases. To study the consistency of the modelled TEC during these phases, we compared the mod-

elled TEC with GPS TEC during the twin solar maxima 2012 and 2014 and solar minima 2017 of the 24th solar cycle over the low-latitude station Pathum Wan.

Monthly variation of VTEC and performance of the IRI mode

From Figure 1 we can observed that IRI-2007, IRI-2012 and IRI-2016 versions show synchronous variation with GPS-derived TEC during the twin solar maxima and solar minima, over the low-latitude station. It was found that the modelled TEC results were a little underestimated compared to the GPS-derived TEC most of the time, but during summer solstice (June–August), the modelled TEC results were little overestimated.

It was also observed that during the twin maxima and minima periods, the IRI-2007 model gave the highest values of TEC compared to the other two versions. It was also observed that the modelled TEC and GPS TEC recorded the highest monthly VTEC during March–April and October, and minimum monthly VTEC during January and July. That is, the modelled TEC and GPS TEC followed a similar sinusoidal pattern with crests in the equinox months and troughs in the solstice months^{25,26}. The ionospheric TEC is controlled by solar photoionization and recombination processes. The sub-solar points move around the equator during the equinoctial period. It can be predicted that the peak in photoelectrons and existence of eastward electric field are potential causes of higher VTEC peaks during equinox. On the other hand, during solstice months, the sub-solar points move up to higher latitudes. Moreover, the change in the direction of neutral winds causes lower peaks in during solstice.

Annual variation of VTEC and performance of the IRI mode

Figure 2 shows the annual variation in GPS-derived TEC and modelled TEC during the twin solar maxima 2012 and 2014 and solar minima 2017 at Pathum Wan. It can be observed from the figure that the model underestimates the TEC values during that period, but the similarity in the shape of the curves exhibits visual synchronization²⁷. Also, the curves reached their trough and crest almost during the same period of time, i.e. a similar sinusoidal pattern was followed by the curves. However, the magnitudes of both modelled TEC and GPS TEC were different. It was noticed that highest annual values of GPS TEC and modelled TEC were obtained during solar maximum 2014 and lowest values were obtained during solar minimum 2017. This is because during solar minima periods, less solar radiation is received by the Earth, which leads to less ionization. While during the solar maxima periods, higher amount of solar radiation is received by the Earth leading to higher ionization.

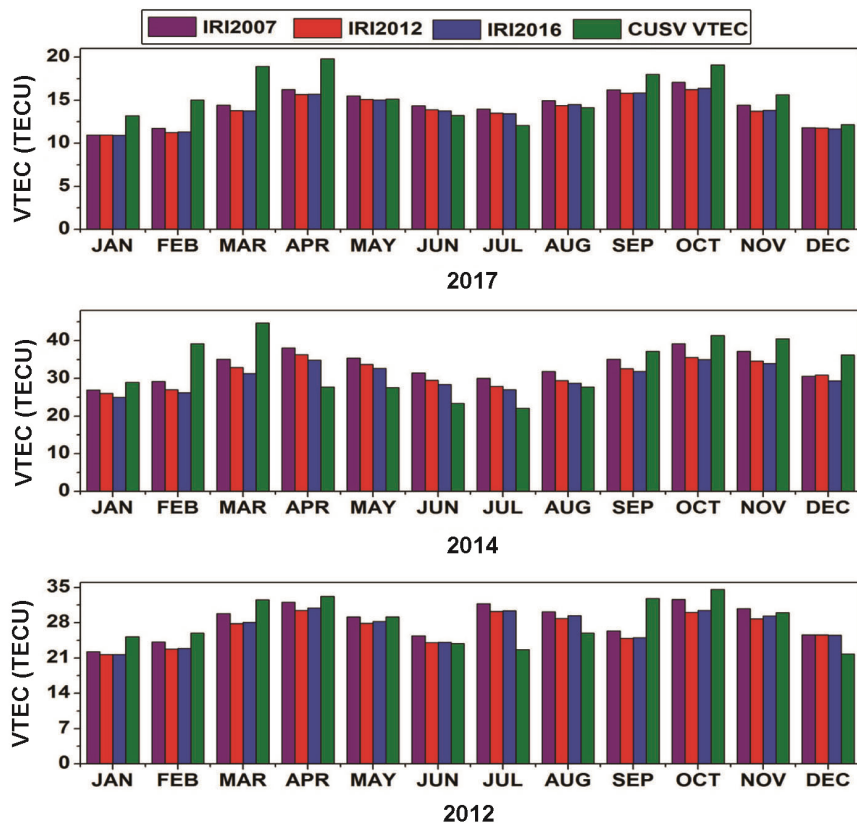


Figure 1. Monthly variability of GPS TEC and modelled TEC during 2012, 2014 and 2017 at the low-latitude station Pathum Wan, Thailand.

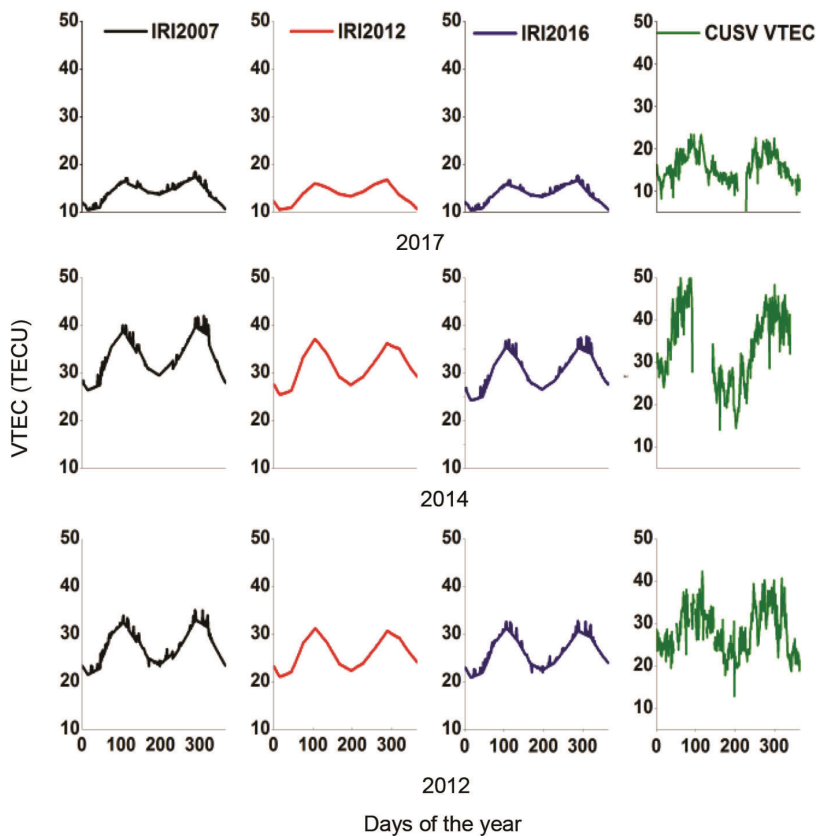


Figure 2. Annual variability of GPS TEC and modelled TEC during 2012, 2014 and 2017 at the low-latitude station Pathum Wan.

Statistical study of the annual variation of modelled TEC with GPS TEC

Figure 3 shows the standard deviation (STD) of the considered IRI versions over Pathum Wan station for 2012, 2014 and 2017. We have statistically analysed daily averaged data and calculated standard deviation of the modelled TEC from the corresponding GPS TEC. From the figure, it can be observed that during twin solar maximum period, the modelled TEC exhibits wider spread range of STD than that of the solar minimum period. The spread range of STD was 0–9 TECU during 2012, 0–16 TECU during 2014 and 0–7 TECU during 2017. It is inferred that the STD spread range is least during the solar minimum 2017. In other words, the STD yields higher numeric values during solar maxima period and lower values during solar minima period. From the analysis, it can be concluded that the IRI model is more suitable when applied during solar minima period.

To quantify the association between GPS TEC and modelled TEC, we statistically analysed daily averaged VTEC data and calculated correlation between modelled TEC and GPS TEC for the twin solar maxima and minima periods (Figure 4). It was observed that GPS TEC and modelled TEC showed a moderate degree of positive correlation during that period. We applied suitable statistical tools and found correlation coefficients between GPS TEC and IRI-2007, IRI-2012 and IRI-2016 to be 0.706, 0.657 and 0.685 respectively, during solar maxima 2012. The correlation coefficients were 0.576, 0.583 and 0.570 respectively, during solar maxima 2014 (ref. 28) and 0.606, 0.570 and 0.579 respectively, during solar minima 2017. From the results, it can be inferred that IRI-2007 is the best version for 2012 and 2017 and the second best version (after IRI-2012) for the year 2014. Broadly, it can be concluded that IRI-2007 is the most suitable version for VTEC studies.

VTEC variation during geomagnetic storms and performance of the IRI model

Geomagnetic storms during solar maxima 2012: It was observed that during the solar maxima 2012, totally 11 storms had occurred. These storms are indicated by $Dst \leq -50$ nT, and also by the southward movement of Bz (or negative values of the Bz component). They all fall in the category of moderate storms. The strongest among these storms occurred on 10 March 2012 (69th day of the year) with Dst -98 nT. These storms are shown by the trough in the Dst graph (Figure 5). We also monitored IMF Bz component during the storm period and observed that its value was -0.1 nT on 7 March 2012. The value dipped suddenly to -4.6 nT on 10 March 2012, indicating strong southward Bz movement. Again during the recovery phase Bz value returned to 0.7 nT on 12 March 2012.

During the storm period, the variability of GPS TEC seems to be connected to the variability of Dst and Bz .

It can be seen from Figure 5 that during the storm period, when Dst dips to a negative value ($Dst \leq -50$ nT), GPS TEC exhibits significant fluctuation. It is also observed that both IRI-2007 and IRI-2016 respond to the geomagnetic storms, as seen from the fluctuation during the storm periods. It can be noticed that IRI-2016 responds better among the considered versions during the solar maximum 2012. On the contrary, the IRI-2012 model gives a smooth curve or registers a very weak response to the storms.

Geomagnetic storms during solar maxima 2014: It was observed that during the solar maxima 2014, three moderate storms had occurred. All the storms are shown by the trough in Dst graph (Figure 6) and also by the southward movement of Bz (or negative values of IMF Bz). The strongest storm occurred on 19 February 2014 (50th day of the year) with Dst -66 nT. We also monitored IMF Bz during the storm period and noted that its value was $+0.6$ nT on 17 February 2014, suddenly which dipped to -1.8 nT on 19 February 2014. This sudden reduction in the positive of IMF Bz and turning it into a negative value indicates Bz movement from northward to southward direction. The southward IMF Bz is primarily responsible for geomagnetic storms. During the storm period, the variability of GPS TEC is connected to the variability of Dst and Bz .

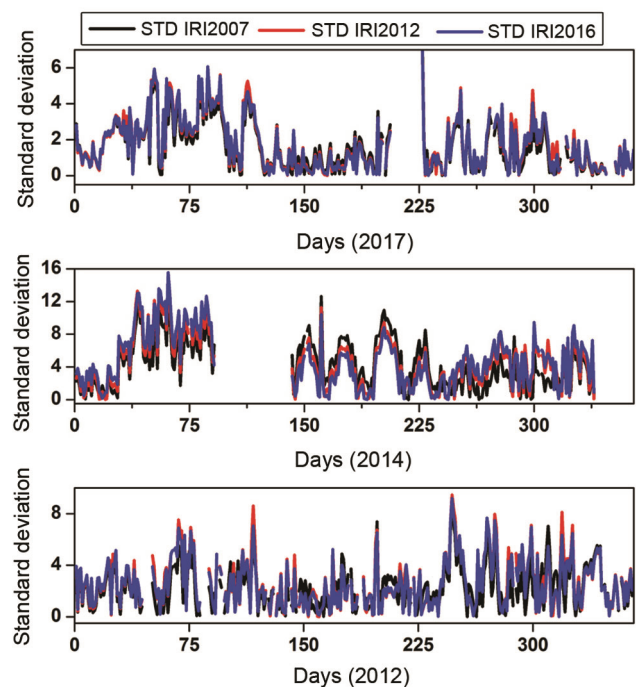


Figure 3. Standard deviation of International Reference Ionosphere (IRI) model from the corresponding GPS TEC over Pathum Wan station for 2012, 2014 and 2017.

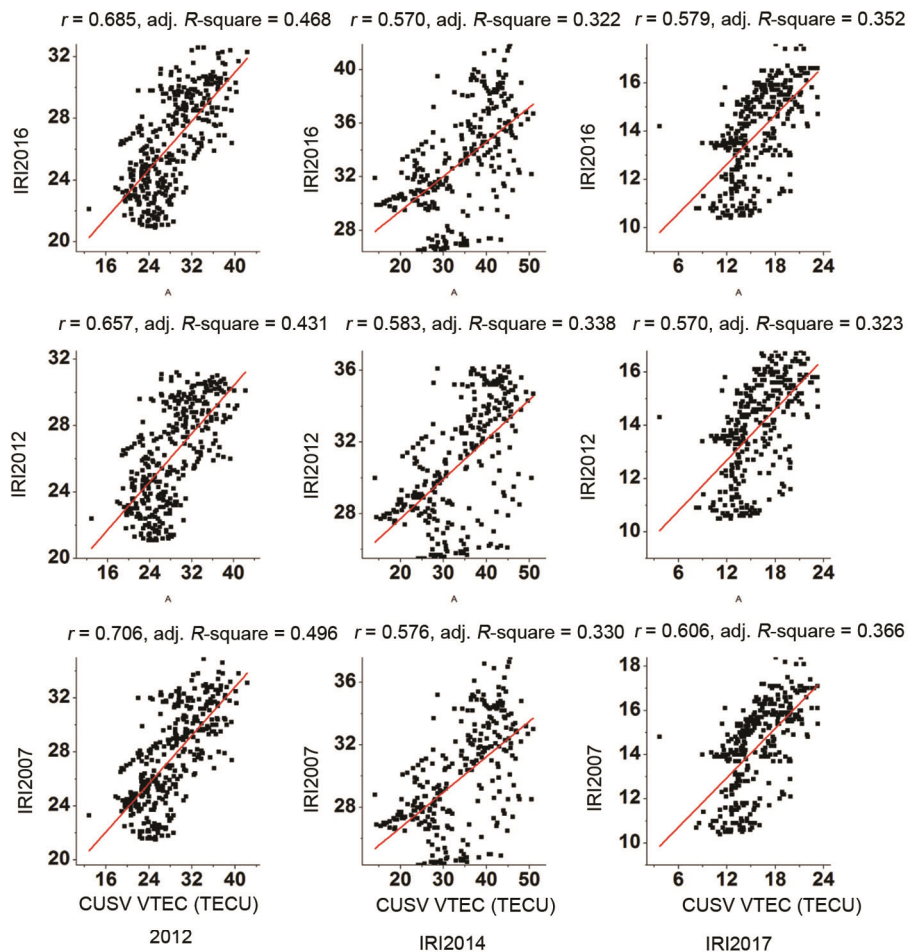


Figure 4. Scatter plot and correlation of GPS TEC with IRI-2007, IRI-2012 and IRI-2016 during 2012, 2014 and 2017.

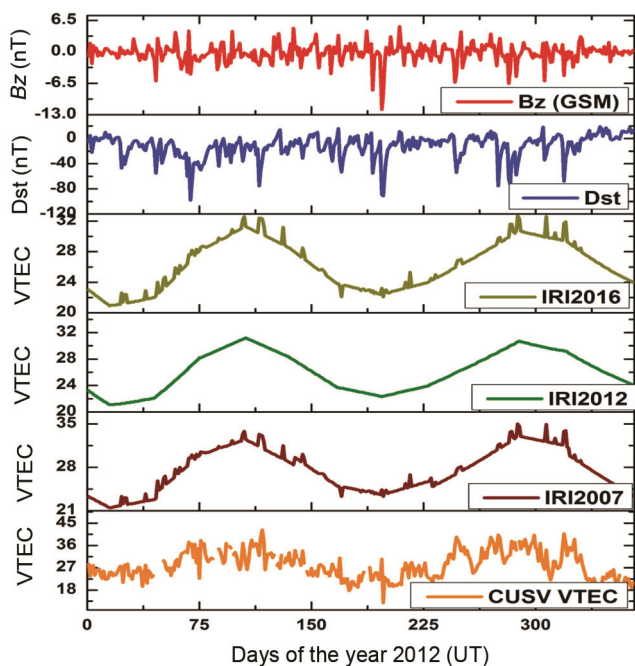


Figure 5. Comparison of variability of GPS TEC and modelled TEC with the geomagnetic indices during solar maxima 2012.

It is clear from Figure 6, that during the storms, when Dst dips to a negative value ($\text{Dst} \leq -50$ nT), GPS TEC and modelled TEC produce significant fluctuations. The fluctuations are more prominent in GPS TEC graphs. It was also observed that both IRI-2007 and IRI-2016 responded to the geomagnetic storms, as observed from the fluctuations during the storm periods. It can be inferred that IRI-2016 responds better than the other versions considered during the solar maximum 2014. It was also noticed that IRI-2012 produced a fluctuation-free curve during the storm period, or it responded poorly to the occurrence of storms.

Geomagnetic storms during solar minima 2017: It was observed that during the solar minima 2017, three moderate and one intense storms, i.e. totally four geomagnetic storms had occurred. They are shown by the trough in Dst graph (Figure 7) and also confirmed by southward movement of Bz (or negative values of the Bz component). An intense storm occurred on 8 September 2017 (251th day of the year) with Dst-107 nT. We also monitored IMF Bz during the storm period and observed that its value was +0.5 nT on 7 September 2017, which suddenly dipped to

-3.2 nT on 8 September 2017, indicating strong southward B_z movement. Again during the recovery phase, the B_z value returned to +0.5 nT on 9 September 2017. The positive value indicates that the B_z component had returned to the northward direction. During the storm period, the variability of GPS TEC seems to be connected to the variability of Dst and B_z . It is clear from the Figure 7 that during storm period, when Dst dips to a negative value ($Dst \leq -50$ nT), GPS TEC exhibits significant fluctuation. From the figure, it can be observed that both IRI-2007 and IRI-2016 respond almost in a similar manner to the geomagnetic storms during the solar minima 2017. Also IRI-2012 produced a fluctuation-free curve during the storm period. In other words, it responded poorly to the occurrence of storms.

Conclusion

We studied the variation of ionospheric TEC and performance of the IRI model during the twin solar maxima 2012 and 2014 and solar minima 2017 of the 24th solar cycle over low-latitude station. The main conclusions drawn from the study are presented as below:

(i) It was observed that the modelled monthly TEC results were underestimated most of the time. It was also observed that during the twin maxima and minima periods, the IRI-2007 model yielded slightly higher values than the other two versions. It was also observed that the modelled TEC and GPS TEC recorded the highest monthly VTEC during March–April and October, and minimum monthly VTEC during January and July. In other words, the modelled TEC and GPS TEC followed a similar pattern with crests in the equinox months and troughs in the solstice months.

(ii) It was found that modelled TEC results were a little underestimated than that of the GPS-derived TEC most of the time. However, during summer solstice (June–August), the modelled TEC results were little overestimated.

(iii) On analysing the annual VTEC data during the study period, it was observed that the model underestimates TEC values during the period, but the similarity in the shape of the curves exhibits visual synchronization. It was observed that the curves achieved their trough and crest almost during the same period of time, i.e. a similar sinusoidal pattern was followed by the curves.

(iv) It was also observed that highest diurnal values of GPS TEC and modelled TEC were obtained during the solar maxima 2014 and lowest diurnal values during the solar minima 2017.

(v) We calculated standard deviation of modelled TEC from the corresponding GPS TEC during the study period. It can be concluded that the IRI model is more suitable when applied during the solar minima period than the solar maxima period.

(vi) We carried out correlation study between modelled TEC and GPS TEC, and obtained a moderate degree of

positive correlation during the study period. It can be concluded that IRI-2007 is most suitable version.

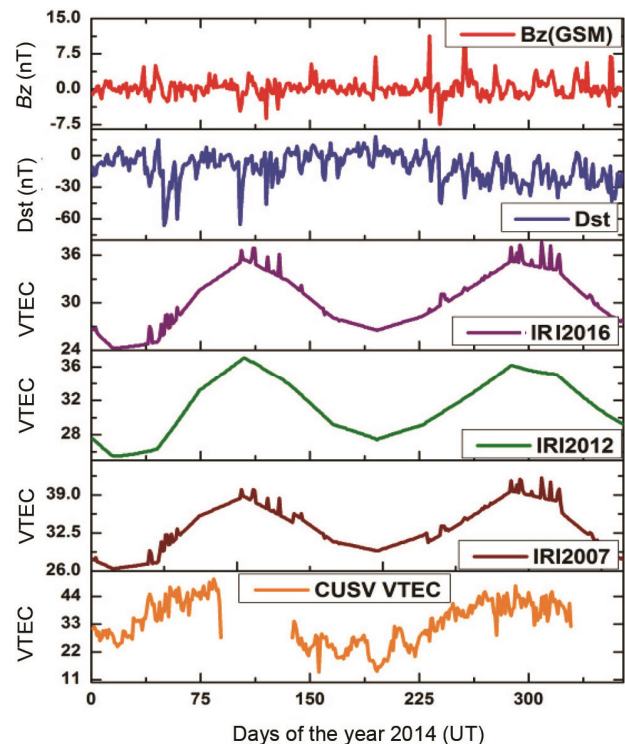


Figure 6. Comparison of variability of GPS TEC and modelled TEC with the geomagnetic indices during solar maxima 2014.

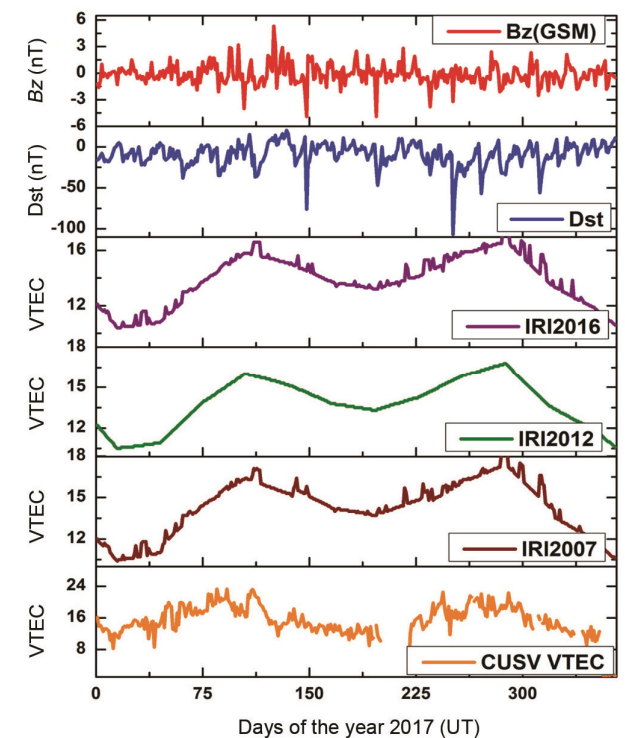


Figure 7. Comparison of variability of GPS TEC and modelled TEC with the geomagnetic indices during solar minima 2017.

(vii) It was observed that during the storm period, the variability of GPS TEC is connected to the variability of Dst and IMF B_z indices.

(viii) Thus it can be concluded that IRI-2016 is most suitable version for TEC estimation, especially during geomagnetic storm periods.

1. Bilitza, D., Hernandez-Pajares, M., Juan, J. M. and Sanz, J., Comparison between IRI and GPS-IGS derived electron content during 1991–97. *Phys. Chem. Earth*, 1999, **24**(4), 311–319.
2. Bilitza, D. and Rawer, K., International reference ionosphere – past, present and future: electron density. *Adv. Space Res.*, 2013, **13**(3), 3–13.
3. Bilitza, D., Lee-Anne, M., Bodo, R. and Tim, F. R., The international reference ionosphere today and in the future. *Geod. J.*, 2011, **85**, 909–920; doi:10.1007/s00190-010-0427.
4. Wang, X., Wan, Q., Maruyama, T., Guanyi, M. A., Jinghua, L. I. and Jiangtao, F., Comparison of global TEC between IRI TEC and GPS TEC in the spring of 2006. In 32nd Union Radio Scientific International General Assembly and Scientific Symposium, Montreal, Canada, 19–26 August 2017.
5. Kelley, M. C., *The Earth's Ionosphere: Plasma Physics and Electrodynamics*, Elsevier, New York, USA, 2009, 2nd edn, p. 545.
6. Hunsucker, R. D. and Hargreaves, R. D., *The High-Latitude Ionosphere and its Effects on Radio Propagation*, Cambridge University Press, Cambridge, UK, 2003.
7. Hofmann-Wellenhof, B., Lichtenegger, H. and Collins, J., *Global Positioning System Theory and Practice*, Springer-Verlag Wien, New York, USA, 1992, pp. 289–311.
8. Misra, P. and Enge, P., *Global Positioning System: Signals, Measurements, and Performance*, Ganga-Jamuna Press, Lincoln, USA, 2006, pp. 200–218.
9. Hansen, A., Blanch, J. T. and Walter, T., Ionospheric correction analysis for WAAS quiet and stormy. In Proceedings of the 13th International Technical Meeting of the Satellite Division of The Institute of Navigation Global Positioning System, Salt Lake City, Utah, USA, 2000, pp. 19–22.
10. Lanyi, G. E. and Roth, T., A comparison of mapped and measured total ionospheric electron content using global positioning system and Beacon satellite observations. *Radio Sci.*, 1988, **23**(4), 483–492.
11. Bilitza, D., International reference ionosphere 2000. *Radio Sci.*, 2001, **36**(2), 261–275.
12. Kumar, S., Tan, E. and Murti, D., Impacts of solar activity on performance of the IRI-2012 model predictions from low to mid latitudes. *Earth Planets Space*, 2015, **67**, 42; doi:10.1186/s40623015-0205-3.
13. Ezquer, R. G. *et al.*, Behaviour of ionospheric magnitudes of F2 region over Tucumán during a deep solar minimum and comparison with the IRI 2012 model predictions. *J. Atmos. Sol.-Terr. Phys.*, 2014, **107**, 89–98.
14. Asmare, Y., Tsgaye, K. and Melssew, N., Validation of IRI-2012 TEC model over Ethiopia during solar minimum (2009) and solar maximum (2013) phases. *Adv. Space Res.*, 2014, **53**, 1582–1594; <http://dx.doi.org/10.1016/j.asr.2014.02.017>.
15. Abdu, M. A., Batista, I. S. and Souza, J. R., An overview of IRI-observational data comparison in American (Brazilian) sector low latitude ionosphere. *Adv. Space Res.*, 1996, **18**(6), 13–22.
16. Kumar, S., Performance of IRI-2012 model during a deep solar minimum and a maximum year over global equatorial regions. *J. Geophys. Res., Space Phys.*, 2016, **121**, 394; doi:10.1002/2015JA022269.
17. Tariku, Y. A., Patterns of GPS-TEC variation over low-latitude region (African sector) during the deep solar minimum (2008 to 2009) and solar maximum (2012 to 2013) phases. *Earth Planets Space*, 2015, **67**, 35; doi:10.1186/s40623-015-0206-2.
18. Tariku, Y. A., Variability of TEC and improvement of performance of the IRI model over Ethiopia during the high solar activity phase. *Ann. Geophys. Discuss.*, 2018, 48; <https://doi.org/10.5194/angeo-2018-48>.
19. Mahesh, P., Roshni, A., Shweta, M. and Purohit, P. K., Latitudinal variation of ionospheric TEC at northern hemispheric region. *Russ. J. Earth Sci.*, 2019, **19**, 1; doi:10.2205/2018ES000644.
20. Olawepo, A. O., Oladipo, O. A., Adeniyi, J. O. and Doherty, P. H., TEC response at two equatorial stations in the African sector to geomagnetic storms. *Adv. Space Res.*, 2015, **56**(1), 19–27.
21. Hamzah, S. Z. M. and Homam, M. J., The correlation between total electron content variations and solar activity. *ARPN J. Eng. Appl. Sci.*, 2015, **10**(20).
22. Bilitza, D. *et al.*, The International Reference Ionosphere 2012 – a model of international collaboration. *J. Space Weather Space Climate*, 2014, **4**, A07.
23. Rush, C., Fox, M. and Bilitza, D., Ionospheric mapping – an update of foF2 coefficients. *Telecommunications J.*, 1989, **56**, 179–182.
24. Aggarwal, M., TEC variability near northern EIA crest and comparison with IRI model. *Adv. Space Res.*, 2011, **48**(7), 1221–1231.
25. Roshni, A., Azad, A. M., Parvaiz, A. K. and Rafi, A., Study of ionospheric TEC variability over low, mid and high latitudes during solar maximum and its comparison with IRI-2012 and IRI-2016 model. *Astronom. Astrophys. Trans.*, 2017, **30**(2), 223–232.
26. Tariq, M. A., Shah, M., Inyurt, S., Shah, M. A. and Liu, L., Comparison of TEC from IRI-2016 and GPS during the low solar activity over Turkey. *Astrophys. Space Sci.*, 2020, **365**, 179.
27. Jumpon, U., Supnithi, P., Phakphisut, W., Hozumi, K. and Tsugawa, T., Assessment of GPS-TEC with the IRI-2016 model, the IRI-Plas model and GIM-TEC during low solar activity at KMITL, Thailand. In 34th International Technical Conference on Circuits/Systems, Computers and Communications. 23–26 June 2019. Date added to IEEE *Xplore*, 12 August 2019; doi:10.1109/ITC-CSCC.2019.8793371.
28. Ghimire, B. D., Chapagain, N. P., Basnet, V., Bhatta, K. and Khadka, B., Variation of GPS-TEC measurements of the year 2014: a comparative study with IRI-2016 model. *JNPS*, 2020, **6**(1), 90–96; doi:<http://doi.org/10.3126/jnphysoc.v6i1.30555>.

ACKNOWLEDGEMENTS. We thank the various on-line data server sites like Scripps Orbit and Permanent Array Center SOPAC (<http://sopac.ucsd.edu/dataArchive/>), Space Physics Data Facility OMNI (<http://omniweb.gsfc.nasa.gov/>), <http://irimodel.gov/> and Dr Gopi Krishna Seemala (Indian Institute of Geomagnetism, Navi Mumbai, India) for freely distributing the software to process raw TEC data.

Received 23 October 2020; revised accepted 2 October 2021

doi: 10.18520/cs/v121/i11/1417-1424